Anal. Chem. **2002,** *74,* 2198−2209

Multicomponent Lifetime-Based pH Sensors Utilizing Constant-Lifetime Probes

William D. Bare, Nathan H. Mack, Wenying Xu, and J. N. Demas*

Department of Chemistry, McCormick Road, University of Virginia, Charlottesville, Virginia 22904

B. A. DeGraff

Department of Chemistry, James Madison University, Harrisonburg, Virginia 22807

A multicomponent luminescent sensor system is described that uses probe species with constant lifetimes to generate an analyte-dependent change in the apparent sensor lifetime. This new sensing scheme not only allows for lifetime-based measurement techniques to be applied to sensors that employ static quenching interactions but also provides the ability to vary the sensitivity of the sensor system with simple changes in instrumental parameters. A model for the multicomponent sensor is presented, followed by data measured using a prototype pH sensor based on the model.

In recent years there has been tremendous growth in the application of luminescence-based analytical techniques. Techniques have been developed for quantitative detection of dozens of analytes including O_2,[1] CO_2,[2] H^+,[3] metal ions,[4] and glucose.[5] These techniques have found use in fields as diverse as aerodynamics[6] and biomedical analysis.[7] A current goal in the field of luminescence-based sensing is to develop probes and instrumentation that allow for lifetime-based measurements that offer important advantages over intensity-based techniques.

In particular, long-lived excited-state transition metal complexes (TMCs) are in the process of revolutionizing many analytical areas. TMCs can have many potential advantages as luminescence probes including long excited-state lifetimes (τ's), falling in the range 0.1−>100 μs, and high luminescence quantum yields in the 0.01−0.7 range. Many TMCs are easily excited in the visible with low-cost LEDs or inexpensive diode lasers. They have large spectral shifts between the excitation and emission, which minimizes the difficulty of isolating the excitation and emission wavelengths. Long τ's make them much easier to measure than the typical low-nanosecond organic probes. Further, long lifetimes allow efficient time discrimination from the ubiquitous fluorescences of short-lived organics or scattering.[8,9]

Many existing luminescent sensor systems rely on a static quenching interaction between the probe and analyte to generate an analyte-dependent change in steady-state luminescence intensity. Steady-state intensity measurements, however, can be adversely affected by fluctuations in excitation source intensity, detector sensitivity, efficiency of optical components, and photodecomposition and are, thus, prone to measurement errors, particularly in small, portable instruments used for on-site applications. For this reason, instrumentation must include a method to obtain a reference signal, resulting in increased complexity and cost. A general approach that has been employed to circumvent problems related to signal drift is the development of probes and instrumentation that allow for lifetime-based measurements, which are not subject to these errors. Unfortunately, systems that employ static quenching are generally not amenable to simple lifetime-based sensing.

Phase fluorometer methods using internal references have been developed for use with statically quenched systems. The method typically uses a long-lived reference molecule and the frequency dependence of the phase and modulation properties for these binary mixtures to quantitate the statically quenched luminophore.[10] In their pristine form, these techniques do not discriminate against scattered light or short-lived fluorescence impurities. One paper gave the concept of using time gating to eliminate these artifacts, but there were no details and no experiments.[10c,e]

This paper describes a new multicomponent sensor system that takes advantage of the intensity changes resulting from static quenching interactions to produce lifetime-based sensors. The

(1) (a) Bacon, J. R.; Demas, J. N. *Anal. Chem.* **1987**, *59*, 2780−2785. (b) Carroway, E. R.; Demas, J. N.; DeGraff, B. A.; Bacon, J. R. *Anal. Chem.* **1991**, *63*, 337−342. (c) Hartmann, P.; Leiner, M. J. P.; Lippitsch, M. E. *Anal. Chem.* **1995**, *67*, 88−93. (d) Rosenzweig, Z.; Kopelman, R. *Anal. Chem.* **1995**, *67*, 2650−2654. (e) Xu, W.; Kneas, K. A.; Demas, J. N.; DeGraff, B. A. *Anal. Chem.* **1996**, *68*, 2605−2609.

(2) (a) Liebch, G.; Klimant, I.; Frank, B.; Holst, G.; Wolfbeis, O. S. *Appl. Spectrosc.* **2000**, *54*, 548−559. (b) Neurater, G.; Klimant, I.; Wolfbeis, O. S. *Anal. Chim. Acta* **1999**, *382*, 67−75.

(3) Thompson, R. B.; Lakowicz, J. R. *Anal. Chem.* **1993**, *65*, 853−856.

(4) (a) Szmacinski, H.; Lakowicz, J. R. *Sens. Actuators, B* **1993**, *11*, 133−143. (b) Grynkiewicz, G.; Poenie, M.; Tsien, R. Y. *J. Biol. Chem.* **1985**, *260*, 340. (c) Akkaya, E. U.; Lakowicz, J. R. *Anal. Biochem.* **1993**, *213*, 285−289. (d) Shortreed, M.; Kopelman, R.; Kuhn, M. *Anal. Chem.* **1996**, *68*, 1414−1418.

(5) Rosenzweig, Z.; Kopelman, R. *Anal. Chem.* **1996**, *68*, 1408−1413.

(6) (a) Demas, J. N.; DeGraff, B. A.; Coleman, P. B. *Anal. Chem.* **1999**, *71*, 793A−800A. (b) Gouterman, M. *J. Chem. Educ.* **1997**, *74*, 697−702.

(7) Taylor, D. L.; Waggoner, A. S.; Murphy, R. E.; Lanni, F.; Birge, R, R. *Applications of Fluorescence in Biomedical Sciences*; Alan R. Liss, Inc.: New York, 1986.

(8) Lakowicz, J. R. *Principles of Fluorescence Spectroscopy*, 2nd ed.; Plenum: New York, 1999; Chapter 8.

(9) (a) Demas, J. N.; DeGraff, B. A. *Anal. Chem.* **1991**, *63*, 829A. (b) Demas, J. N.; DeGraff, B. A. *Coord. Chem. Rev.* **2001**, *211*, 317−351.

10.1021/ac0110799 CCC: $22.00
Published on Web 04/03/2002

sensors exhibit an analyte-dependent lifetime response, even though the lifetimes of their individual components do not change. A model for the sensor system is presented, the theory of the conditions for optimal sensitivity are discussed, and the method is applied to pH sensors in solution and in polymer supports. The method implemented here uses pulsed measurements with two long-lived species and discriminates completely against scatter and short-lived fluroescences.

THEORY

Static Quenching. Since the technique described herein is specifically applicable to systems based on static quenching, we show the mechanism and mathematical relationships pertinent to these systems. In a static quenching system, the free luminescent probe molecules (P) exist in equilibrium with the analyte (A) and the probe−analyte complex (PA) governed by a stability constant (K_s) as described in eq 1. In the typical case, the free

$$P + A \overset{K_s}{\longleftrightarrow} PA \tag{1}$$

probe is luminescent and the bound form is highly quenched, although some sensing systems work in the opposite fashion; thus, the steady-state emission intensity exhibits an analyte dependence resulting from the changes in the relative concentrations of the free and bound forms of the probe.

$$I = I_0\left(\frac{1}{1 + 10^{(\log[\mathrm{A}] - \mathrm{p}K_s)}}\right) \tag{2}$$

where I and I_0 are the steady-state emission intensities in the presence and absence of the analyte, respectively. This relationship demonstrates that the greatest change in emission intensity (i.e., greatest sensitivity) occurs when the log of analyte concentration is approximately equal to pK_s. The concentration range of useful sensitivity extends ~1 order of magnitude on either side of this point.

A defining characteristic of the static quenching model is that the complex, PA, is kinetically stable relative to the excited-state lifetime, so P, A, and PA may be considered to be noninteracting species during the emission decay. As a result, the emission lifetime is not affected by the analyte concentration, and standard simple lifetime-based measurement techniques cannot be applied to these sensors, although some more elaborate lifetime measurement schemes have been applied.[10]

Although the emission decay generated by a delta pulse excitation for a static quenching probe exhibits a single lifetime, the initial intensity (preexponential factor, α) does vary with analyte concentration, tracking the concentration of the emissive species. The emission decay generated by a delta pulse excitation as a function of time and analyte concentration is given by eqs 3 and 4 in which τ is the excited-state lifetime and α_A and α_0 represent the value of the preexponential factor in the presence and absence of the analyte.

$$I(t,[\mathrm{A}]) = \alpha_A \exp(-t/\tau) \tag{3}$$

$$\alpha_A = \alpha_0\left(\frac{1}{1 + 10^{(\log[\mathrm{A}] - \mathrm{p}K_s)}}\right) \tag{4}$$

Apparent Lifetimes in Systems with Multiexponential Decays. Although pure samples containing a single emissive species are expected to produce simple first-order emission decays, there are several factors (e.g., trace contamination, scattered light, matrix effects in polymer supports, and others) that cause observed decays to be multiexponential. As a result, any attempt to apply luminescence techniques to sensing technology must consider emission decays using a general multiexponential model, as described by eq 5. A potential problem to be

$$I(t) = \sum_{i=1}^{n} \alpha_i \exp(-t/\tau_i) \tag{5}$$

overcome in the development of lifetime-based sensors, therefore, is the multiexponential nature of the observed decays, which complicates their characterization by a single lifetime parameter.

The analysis of a multiexponential decay generates a set of lifetimes (τ_1, τ_2, ...τ_n) and associated preexponential factors (α_1, α_2, ...α_n), and although these data may be useful in describing complex photophysical behavior, they are not desirable for an end-use sensor system. For this purpose, it is necessary to describe the observed emission decay with a *single* lifetime parameter, τ', which varies monotonically with [A]. It has been common to use preexponential-weighted lifetimes (τ_{PE}) or mean lifetimes (τ_m) in these circumstances. For the current application, rapid lifetime determination (RLD) lifetimes (τ_{RLD}) and phase shift lifetimes (τ_{PS}) are believed to be more appropriate. The characteristics of these lifetime definitions are summarized in Table 1, and the RLD method, which is the focus of this paper, is discussed more fully below. Both the RLD and phase shift methods reduce a complex decay curve to a single, generally monotonically varying, apparent lifetime.

The RLD method, shown schematically in Figure 1, circumvents the measurement and analysis of complete decay curves. In a rapid lifetime determination, a fast CCD camera or similar device is used to record the integrated intensity during two consecutive time intervals of the emission decay. Instead of recording an entire decay, this method requires only two measured values, which are the integrated areas under the decay curve for each of the intervals. For a pure single-exponential decay, the lifetime may be determined from the two areas by eq 6, in which

$$\tau_{RLD} = \frac{\Delta t}{\ln(A_1/A_2)} \tag{6}$$

A_1 and A_2 are the integrated areas and Δt is the time interval of

(10) (a) Lakowicz, J. R.; Gryczynski, I.; Gryczynski, Z.; Johnson, M. L. *Anal. Biochem.* **2000**, *277*, 74−85. (b) Lakowicz, J. R.; Castellano, F. N.; Dattelbaum, J. D.; Tolosa, L.; Rao, G.; Grynczynski, I. *Anal. Chem.* **1998**, *70*, 5115−5121. (c) Klimant, L.; Liebsch, G.; Neurauter, G.; Stanglemayer, A.; Wolfbeis, O. S. *New Trends in Fluorescence Spectrcopy: Applications to Chemical and Life Science*; Valeur, B., Brochon, J. C., Eds.; Springer-Verlag: Berlin, Germany, 2001; pp 257−274. (d) Lakowicz, J. R.; Gryczynski, I.; Saxe, S. A. Patent WO 00/14515, March 2000. (e) Lakowicz, J. R. Patent WO 99/60385, November, 1999. (e) Klimant, I. Patent WO 99/06821. February 1999.

Table 1. Definitions and Characteristics of Various Lifetimes Applied to Multiexponential Decays

lifetime	abbrev	definition	comments
preexponential-weighted lifetime	τ_{PE}	$\tau_{PE} = \frac{\sum_{i=1}^{n} \alpha_i \tau_i}{\sum_{i=1}^{n} \alpha_i}$	tends to overweight short-lived components and is highly susceptible to errors caused by scattered light
mean lifetime	τ_m	$\tau_m = \frac{\sum_{i=1}^{n} \alpha_i \tau_i^2}{\sum_{i=1}^{n} \alpha_i \tau_i}$	tends to overweight long-lived components and is susceptible to errors caused by sloping instrumental baselines
apparent phase shift lifetime	τ_{APS}	$\tau_{APS} = \frac{\sum_{i=1}^{n} \alpha_i \tau_i^2/(1+\omega^2\tau_i^2)}{\sum_{i=1}^{n} \alpha_i \tau_i/(1+\omega^2\tau_i^2)}$	tends to overweight long-lived components for low-frequency measurements and short-lived components for high-frequency measurements
rapid lifetime determination method	τ_{RLD}	$\tau_{RLD} = \frac{\Delta t}{\ln(A_1/A_2)}$	tends to overweight long-lived components for long gate time and short-lived components for short gate times

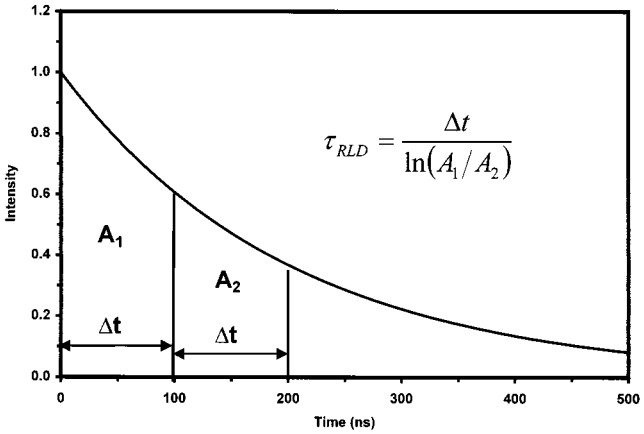

Figure 1. Schematic showing the integrated intensities for lifetime calculations in the rapid lifetime determination method.

the integration or "gate time".[11,12] Areas 1 and 2 can be measured directly (e.g., with a gated CCD camera) or can be computed (following an analysis of the decay curve) from a set of (α_i, τ_i) parameters using eqs 7 and 8. For multiexponential decays, the

$$A_1 = \sum_{i=1}^{n} \int_0^{\Delta t} \alpha_i \exp(-t/\tau_i)\, dt \quad (7)$$

$$A_2 = \sum_{i=1}^{n} \int_{\Delta t}^{2\Delta t} \alpha_i \exp(-t/\tau_i)\, dt \quad (8)$$

apparent lifetime determined by the RLD method (τ_{ARLD} = apparent RLD) is a weighted average of all lifetime components for which the weighting factors depend on both the preexponential factors and the gate time (Δt). Short gate times give more weight to short-lived components, while longer gates preferentially weight the long-lived components. Therefore, for multiexponential decays, the apparent lifetime is dependent upon the gate time.

One advantage of using apparent RLD and phase shift lifetimes is that it gives an indication of the apparent lifetime that would likely be measured in an operational sensor system. The measurement and analysis of complete decay curves is useful in elucidating photophysical processes but is too time-consuming for use in an applied sensor. Marketable sensor systems typically use RLD, phase shift, or similar methods for lifetime-based measurements [2,14] since these methods generate lifetime data without the necessity of nonlinear least-squares fitting of emission decay curves. Recent work[15,16] has indicated that the RLD method may be made even more useful by the employment of overlapping or unequal gate times, resulting in dramatic increases in signal-to-noise ratios.

Real-world probes are expected to give multiexponential emission decays for which a single lifetime parameter must be assigned in order for them to function as useful lifetime-based probes. Four "apparent" or "effective" single-value lifetimes (τ_{PE}, τ_m, τ_{ARLD}, τ_{APS}) have been defined and may be used to describe multiexponential decays with a single lifetime parameter. Each of these may be useful in certain circumstances, although τ_{ARLD} and τ_{APS} are likely to be the most useful for describing the behavior of lifetime-based chemical sensors.

Model for Two-Dye Lifetime-Based Sensors. In a complex emission decay, a change in apparent lifetime can be brought about either by causing a change in the lifetime of one or more components or by causing a change in the relative weights applied to each component, as indicated in eqs 6−8 and those in Table 1.

(11) Woods, R. J.; Scypinski, S.; Love, L. J. C.; Ashworth, H. A. *Anal. Chem.* **1984**, *56*, 1395.
(12) Ballew, R. M.; Demas, J. N. *Anal. Chem.* **1989**, *61*, 30−33.
(13) Szmacinski, H.; Lakowicz, J. R. *Anal. Chem.* **1993**, *65*, 1668−1674.
(14) Szmacindki, H.; Chang, Q. *Appl. Spectrosc.* **2000**, *54*, 106−109.
(15) Sharman, K. K.; Periasamy, A.; Ashworth, H.; Demas, J. N.; Snow, N. H. *Anal. Chem.* **1999**, *71*, 947−952.
(16) Chan, S. P.; Fuller, Z. J.; Demas, J. N.; DeGraff, B. A. *Anal. Chem.* **2001**, *73*, 4486-4490.

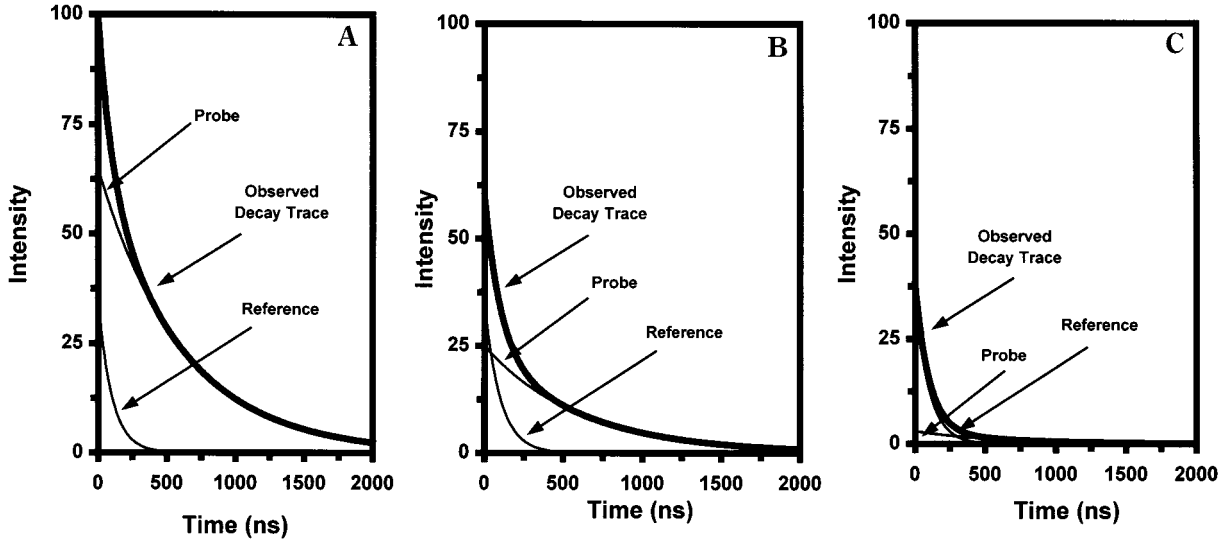

Figure 2. Modeled emission decay curves at different analyte concentrations. Emission decay at (A) low, (B), intermediate, and (C) high [A]. The observed emission decay (which is the sum of the emission of the probe and reference species) shows a change in its apparent lifetime although the lifetimes of the probe and reference species exhibit constant lifetimes.

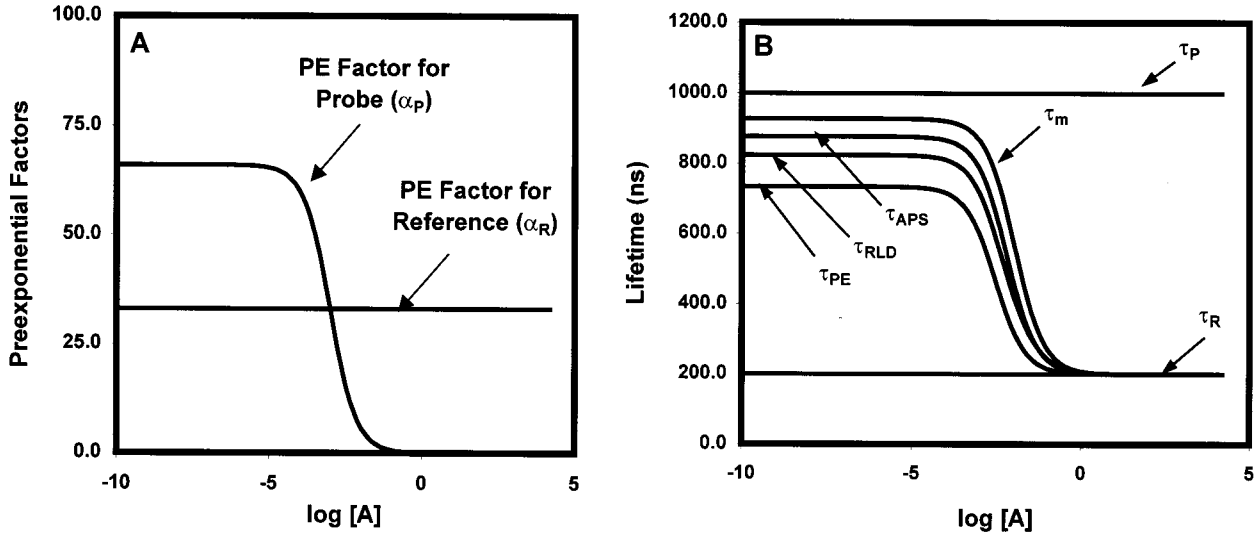

Figure 3. (A) Preexponential factors of the probe and reference species as a function of analyte concentration for a two-component sensor in which the probe species interacts via static quenching ($K_S = 1000$) and is described by eq 4. (B) Lifetimes of the probe and reference species and calculated single-value lifetimes for the mixture as a function of analyte concentration. The gate time used for the RLD calculations was 600 ns, and the modulation frequency for phase shift lifetimes was 20 kHz.

The system described here takes the latter approach, using unquenched reference luminophores to create lifetime-based static quenching sensors.

The principle of affecting a change in the apparent lifetime of a multicomponent decay by varying the weights applied to each component is demonstrated in Figure 2. This figure shows the modeled behavior of a complex emission decay resulting from a combination of two luminophores in solutions of varying analyte concentration. One species, the "reference" ($\tau = 200$ ns), exhibits photophysical behavior, which does not depend on analyte concentration and generates the same emission decay in all three modeled curves. The second component, the "probe" ($\tau = 1000$ ns), interacts with the analyte and exhibits a change in intensity, but not in lifetime, according to the static quenching model (eqs 3 and 4). In solutions of low analyte concentration (Figure 2A), the probe is predominantly in the free form and is the major contributor to the overall emission decay curve, with the apparent lifetime of the combined decay close to that of the probe alone. In a solution with high analyte concentration (Figure 2C), the relative contributions are reversed, and the apparent lifetime for the decay curve approaches that of the reference. At an intermediate analyte concentration (Figure 2B), both species make a significant contribution to the total emission decay, and the apparent lifetime falls near the mean of the probe and reference species.

The change in apparent lifetime that would be observed for this model system is shown in Figure 3. Figure 3A shows the variation of the preexponential factors of each component as a function of analyte concentration. The preexponential factor for the probe (α_P) varies as a function of analyte concentration, as described by eq 4. The preexponential factor for the reference (α_R) is a constant.

Figure 3B shows the modeled lifetimes of the probe and reference species and the resulting apparent lifetimes arising from the analyte-dependent change in α_P for this system. Lifetimes were all calculated from eqs 6−8 and those in Table 1. Each of these apparent lifetimes (i.e., τ_{PE}, τ_m, τ_{ARLD}, and τ_{APS}) has a different dependence on measurement parameters; however, in all cases, the apparent lifetimes show a monotonic change as a function of analyte concentration, with inflection points near the pK_s of the probe−analyte equilibrium. In this model, the probe species (τ = 1000 ns) was longer-lived than the reference species (τ = 200 ns), although the model in which the relative lifetimes are reversed produces analogous results.

Thus, luminescent probes that utilize static quenching interactions in conjunction with an analyte-independent reference can be made to exhibit an analyte-dependent change in apparent lifetime. This allows these probe species to utilize lifetime-based measurement schemes and thereby avoid problems associated with steady-state intensity measurements. A two-component, phase shift sensor system using an unreactive reference molecule was reported for a chloride sensor.[17] In contrast to our system, this method employs a short-lifetime sensor molecule. A disadvantage of this scheme is that it cannot discriminate against scatter or short-lived impurities. Our RLD method with long-lived reference and probe species can be easily gated to effectively eliminate these interferences. Because the two most commonly employed lifetime definitions are instrument parameter-dependent, we explore the effects of the more frequently adjusted parameters on the apparent lifetimes.

Effect of Instrumental Parameters on Sensitivity. For both RLD and phase shift methods, the observed apparent lifetime is a function of measurement parameters with short gate times (or high modulation frequencies) overweighting short-lived components and long gate times (or low modulation frequencies) overweighting long-lived components. For multicomponent sensors, this dependence affects not only the apparent lifetimes but also the sensitivity and apparent inflection points in the analyte response curve. Thus, the variation of instrumental parameters can be used to adjust the sensitivity range of a sensor according to analytical needs. The effect of instrumental parameters on measurement sensitivity is considered here for the RLD method. A system similar to that described here, but using a very short-lived probe, has been described[17] and the authors have discussed the optimum frequencies for use in phase shift measurements.

There are too many variables to consider all cases explicitly; however, one example will provide an illustration of the important points. Figure 4A shows the effect of gate time on the observed RLD lifetime for a hypothetical two-component sensor in solution. For this example, lifetimes of 100 and 1000 ns were chosen for the reference and probe species, respectively, and the ratio of preexponential factors for the probe and reference species is 5:1 in the absence of analyte. The preexponential factor of the probe species decreases with increasing analyte concentration, according to eq 4, with a pK_s of −3. RLD lifetimes were calculated from eqs 6−8. There is a monotonic change in τ_{ARLD} as the relative contribution of the reference and probe species change. One should note that at high [A] only one species (the reference)

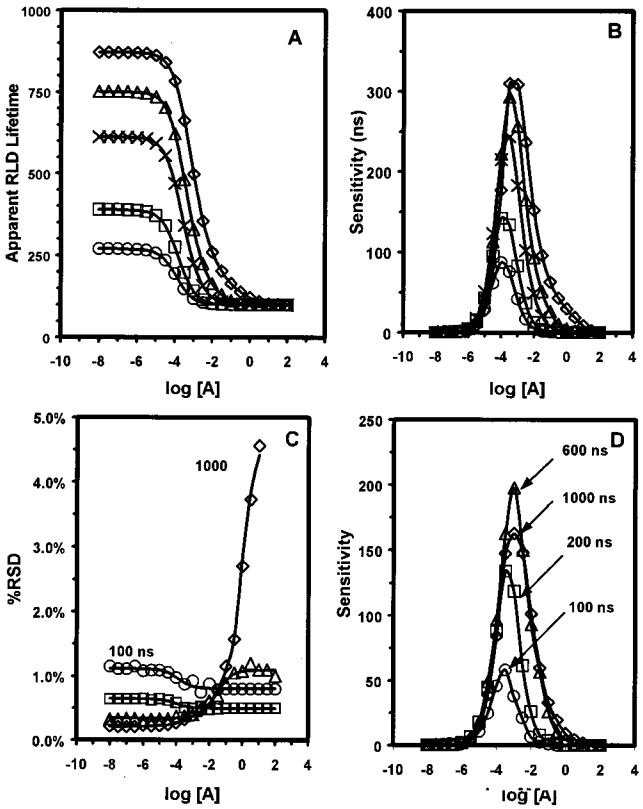

Figure 4. Four plots showing the effect of measurement parameters on lifetime determinations for two-component sensors, using the RLD method: (A) liftimes; (B) theoretical sensitivity; (C) relative standard deviation; (D) analytical sensitivity. The data in these plots were obtained from a Monte Carlo simulation with 10^6 total photons at low [A] (photon count decreases with increasing analyte concentration), pK_s = −3.0, τ_R = 100 ns, τ_P = 1000 ns, and α_R = 0.2, α_P defined by eq 4 with a maximum value of 0.8. Gate times were as follows: (○) 100, (□) 200, (×) 400, (△) 600, and (◇) 1000 ns. Some data sets were omitted in some plots for clarity.

contributes to the emission. Under this condition, the decay approaches a single exponential, and the apparent lifetime exhibits no gate dependence. At low [A], however, the decay is multiexponential, and the apparent lifetime is strongly dependent upon the gate time, as described above. Thus, gate times affect not only individual measured lifetimes but also the maximum possible change in lifetime that can be observed over a range of analyte concentration.

The greatest sensitivity that can be expected, the theoretical sensitivity (S_{Th}), has been defined as the absolute value of the slope of the response curve as in eq 9.[18] The theoretical sensitivity

$$S_{Th}([A]) = \left|\frac{\Delta\tau}{\Delta[A]}\right| \qquad (9)$$

for apparent RLD lifetimes for this modeled sensor is shown in Figure 4B. This plot shows that absolute sensitivity and concentration of maximum sensitivity are also affected by gate width. For this reason, a particular two-component sensor may be tuned by judicious variation of instrumental parameters.

(17) Huber, C.; Klimant, I.; Krause, C.; Wolfbeis, O. S. *Anal. Chem.* **2001**, *73*, 2097−2103.

(18) Skoog, D. A.; Leary, J. J. *Principles of Instrumental Analysis*, 4th ed.; Saunders College Publishers: Fort Worth, TX, 1992; p 7.

Table 2. Ligand Structures and Abbreviations

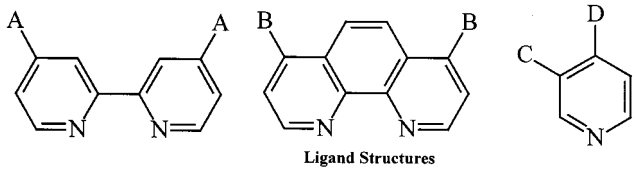

Ligand Structures

abbreviation	name	structure	
bpy	2,2′-bipyridine	A = H	
t-but$_2$bpy	4,4′-bis(*tert*-butyl)−2,2′-bipyridine	A = C(CH$_3$)$_3$	
phen	1,10-phenanthroline	B = H	
$\phi_2$phen	4,7-diphenyl-1,10-phenanthroline	B = C$_6$H$_5$	
py	pyridine	C = H	D = H
py-3-OH	3-hydroxypyridine	C = OH	D = H
py-3-NH$_2$	3-aminopyridine	C = NH$_2$	D = H
ppp	4-(3-phenylpropyl)pyridine	C = H	D = (CH$_2$)$_3$C$_6$H$_5$

To predict the actual sensitivity that is to be expected, however, one must also consider the standard deviation associated with measurements under each set of instrumental conditions. Analytical sensitivity (S_{Anal}) has been defined[18] as the theoretical sensitivity divided by the standard deviation of measurements, as shown in eq 10. For RLD measurements of single-exponential decays, it

$$S_{Anal}([A]) = \left(\frac{S_{Th}([A])}{\text{Std Dev}([A])}\right) \qquad (10)$$

has been shown that the standard deviation is a minimum when the gate width is ∼3 times larger than the lifetime.[12,15] For two-component sensors, however, this relationship is much more complicated because both the apparent lifetime and total number of photons change as a function of analyte concentration. A Monte Carlo simulation[12,15,16] was performed to determine the expected standard deviation for the model system under consideration. The results of this simulation are shown in Figure 4C, and the parameters employed in the simulation are provided in the figure caption. This figure shows the results of opposing factors contributing to the measurement's precision. Larger gate times utilize a greater fraction of the emission decay, thus collecting more photons and generating data with better precision (as is seen in the region of low analyte concentration). However, this effect may be offset in conditions where the long-lived component is highly quenched. In this case, at high analyte concentration, only the short-lived (100 ns) reference species contributes to the signal. Thus, for long gate times, few photons are collected in the second integration area. The low photon counts in the second integration area result in large standard deviations in the calculated lifetimes.

Finally, the predicted analytical sensitivity, as defined by eq 10, is shown in Figure 4D. This figure shows the combined effects of changes in theoretical sensitivity and expected measurement precision. The number of variable parameters (α_R, $\alpha_{P,max}$, τ_R, τ_P, Δt) is too large to permit a concise mathematical summary of these effects, and a detailed discussion would be well beyond the scope of the current paper. However, it is generally the case that the greatest sensitivity is obtained when α_P (in the absence of analyte) is several times greater than α_R and Δt is near the mean of τ_P and τ_R.

The utility of this sensing technique has been demonstrated by a prototype pH sensor, for which data are presented below. We turn now to real systems.

EXPERIMENTAL SECTION

Materials. Rhenium complexes of the form Re(CO)$_3$(NN)Cl and Re(CO)$_3$(NN)(L)ClO$_4$ (where NN is 2,2′-bipyridine, 1,10-phenanthroline, or a substituted derivative and L is pyridine or a substituted derivative) were prepared following published procedures.[19] General molecular structures and ligand abbreviations are provided in Table 2. Purity of complexes was checked by elemental analysis or by the method of relative excitation spectra.[20] Elemental analyses agreed to within 1% and ratioed excitation spectra were flat to within 3%.

Luminescent rhenium complexes containing the hydroxypyridine ligand have been shown to exhibit a pH-dependent intensity response, which is analogous to static quenching.[21] For these complexes, the protonated form is luminescent, and the deprotonated form is nonluminescent at room temperature. As a result, a single lifetime is observed, although the steady-state intensity and emission decay profiles are pH-dependent as described by eqs 11 and 12, which are modified (with pH replacing log[A] and

$$I = I_{max}\left(\frac{1}{1 + 10^{(pH - pK_a)}}\right) \qquad (11)$$

$$\alpha = \alpha_{max}\left(\frac{1}{1 + 10^{(pH - pK_a)}}\right) \qquad (12)$$

pK_a replacing pK_s) versions of eqs 2 and 4. The long-range goal of much sensor research is the production of polymer-supported sensor systems; therefore, we developed and investigated the performance of the two-component sensors in polymer supports. The polymer material that was used for these studies was D4J2000,

(19) Sacksteder, L.; Zipp, A. P.; Brown, E. A.; Streich, J.; Demas, J. N.; DeGraff, B. A. *Inorg. Chem.* **1990**, *29*, 4335−4340.

(20) Sacksteder, L.; Demas, J. N.; DeGraff, B. A. *Inorg. Chem.* **1989**, *28*, 1787−1792.

(21) (a) Bare, W. D. Ph.D. Thesis, University of Virginia, 2001; Chapter 9. (b) Bare, W. D.; Mack, N. H.; Demas, J. N.; DeGraff, B. A. *Proc. SPIE* **2001**, *4199*, 1−7. (c) Bare, W. D.; Mack, N. H.; Demas, J. N. *J. Fluoresc.* Manuscript in Preparation.

Table 3. Doping Solutions Used for Construction of pH Sensors

components	function	concentration in doping solution
	Sensor 1	
$Re(CO)_3(t\text{-but}_2bpy)(py\text{-}3\text{-}OH)ClO_4$	short-lived probe	0.4 mg/10 mL
$Re(CO)_3(\phi_2phen)(ppp)ClO_4$	long-lived reference	0.2 mg/10 mL
	Sensor 2	
$Re(CO)_3(\phi_2phen)(py\text{-}3\text{-}OH)ClO_4$	long-lived probe	0.2 mg/10 mL
$Re(CO)_3(t\text{-but}_2bpy)Cl$	short-lived reference	0.5 mg/10 mL

synthesized as described previously.[22] This network polymer was chosen for its amphiphilic properties, which are essential for pH measurements. The polymer is composed of nonpolar siloxane rings, which are connected by long polyether chains. The nonpolar region provides a binding site for organometallic luminescent probe species, while the polar cross-linker allows for absorption of water and free diffusion of protons to and from the sensor species. The utility of this polymer as a support for luminescent transition metal pH sensors was demonstrated by Clarke and coworkers.[23]

Preparation of Samples. Following the two-component sensor model outlined above, an aqueous solution containing a mixture of two luminescent rhenium complexes was prepared. This mixture contained $Re(CO)_3(phen)(py\text{-}3\text{-}OH)ClO_4$ (τ = 555 ns) and $Re(CO)_3(phen)(py\text{-}3\text{-}NH_2)ClO_4$ (τ = 135 ns), which serve as the pH-dependent and pH-independent species, respectively. The effective pK_a of $Re(CO)_3(phen)(py\text{-}3\text{-}OH)ClO_4$ is 6.8. Although the aminopyridine complex contains a protonatable site, this species exhibits pH-independent emission intensity and lifetime over the pH range 2−11.[21] Ethanol (20%) was added to the solution to ensure solubility of the complexes over the entire pH range studied.

Single-dye polymer samples were prepared as follows. Small (∼8 mm × 8 mm × 2 mm; ∼30 mg) pieces of solid polymer material were each placed in a solution of a luminescent rhenium complex (∼0.6 mg complex/10 mL of solution; 0.005 wt %) in methylene chloride. The polymer and solution were continuously agitated in a sealed vial on a mechanical shaker on low speed for 2−4 h. During shaking, the polymer swells, allowing infusion of the rhenium dye. The doped polymers were sliced laterally with a razor blade to yield two thinner (1 mm) polymer pieces. The thinner samples exhibit shorter equilibration times and generate more reproducible data. After cutting, the polymer samples were washed with ethanol to remove dye molecules adhering to the surface and were then slowly air-dried in a methylene chloride atmosphere. During drying, the solvent evaporates, leaving the rhenium complex in the pores of the polymer matrix. Polymers were then dried for several hours under vacuum. The dried polymer samples were placed in 5% aqueous ethanol and shaken for 24 h to ensure that the complexes do not leach from the polymer. No luminescence was observed in the ethanol wash solutions for any of these samples. Finally, the polymers were shaken in water for several hours to remove absorbed ethanol.

Measurements of the mass of methylene chloride solution before and after shaking indicate that the polymer absorbs a quantity of solvent approximately equal to 19 times its own weight. On the basis of this measurement, we conclude that the doped polymers contained ∼0.1 wt % luminescent dye.

Finally, polymers were also doped with mixtures of pH-dependent and pH-independent luminophores to function as probe and reference species in prototype polymer-supported pH sensors. The mixed luminophore sensors were produced in the same way as described above for the single-species doped polymers, except that the doping solutions contained a mixture of luminophores, as described in Table 3. Sensor 1 couples a short-lived probe with a long-lived reference, while sensor 2 pairs a long-lived probe with a short-lived reference.

Measurement of Sample Emission Properties. Solution-phase samples were analyzed by performing a lifetime-based pH titration, as described previously.[24] Briefly, this technique employs an automated titration apparatus to gradually vary the solution pH across a wide range while holding the concentration of all luminescent species constant. At regular pH intervals, the sample is excited with a pulsed nitrogen laser, and the emission decay curve is recorded on a digital oscilloscope (Tektronix TDS 540). This process allowed for the collection of dozens of decay curves over the pH range 2−11. Each decay curve was subsequently analyzed by nonlinear least-squares fitting to generate a set of (α_i, τ_i) parameters consistent with the multiexponential model described by eq 5.

Emission properties of doped polymer samples were measured with the polymers submerged in aqueous solutions of measured pH. Aqueous solutions of HCl and NaOH were prepared at pH 2 and 12. The ionic strength of each was adjusted to 0.1 M with NaCl, and a small amount of $H_2PO_4^-/HPO_4^{2-}$ buffer (total concentration, 100 μM) was added to stabilize pH measurements near the neutral point. Polymer pieces were placed in ∼10 mL of either the acidic or basic solution in a stoppered vial and were shaken (mechanical shaker on lowest speed) for 2 h prior to the first measurement. The pH of the solution was measured, and the polymer piece was transferred with an aliquot of the solution to a quartz cuvette. The polymer sample was positioned against the inside surface of the front face of the cuvette, and emission spectra and emission decay curves were recorded. Emission spectra were recorded on a SPEX Fluorolog 1680 instrument, using front face illumination. Emission decay curves were recorded in the same cuvette, using the pulsed nitrogen laser and a digital oscilloscope used for solution-phase samples.

Following each measurement, the polymer samples were returned to the vial and acidic or basic solution was added to the sample to adjust the pH, and the process described above was

(22) Xu, W.; McDonough, R. C.; Langsdorf, B.; Demas, J. N.; DeGraff, B. A. *Anal. Chem.* **1994**, *66*, 4133−4141.

(23) Clarke, Y. M.; Xu, W.; Demas, J. N. *Anal. Chem.* **2000**, *72*, 3468−3475.

(24) Mack, N. H.; Bare, W. D.; Demas, J. N.; DeGraff, B. A. *J. Fluoresc.* **2001**, *11*, 113−118.

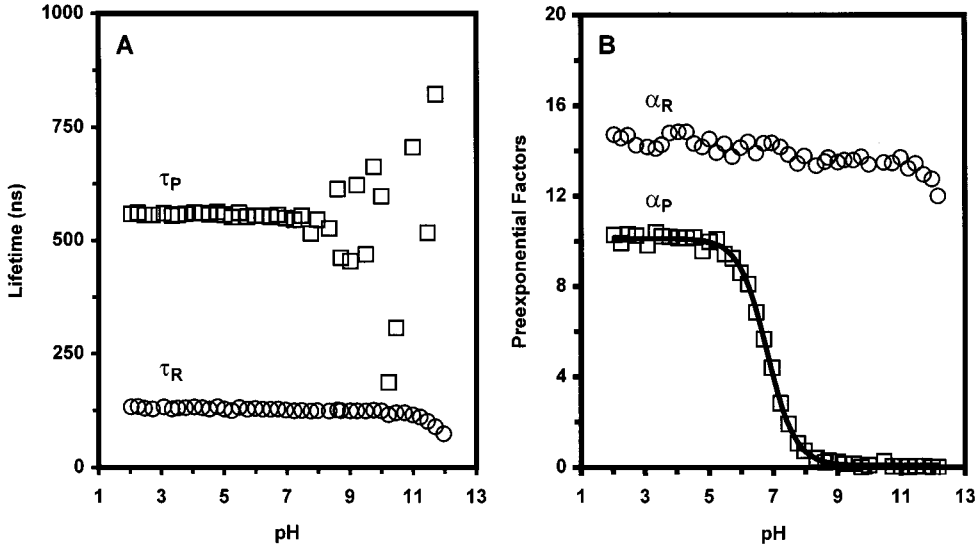

Figure 5. Measured lifetimes (A) and preexponential factors (B) for a solution-phase mixture of two luminophores. Probe, $Re(CO)_3(phen)(py\text{-}3\text{-}OH)ClO_4$; reference, $Re(CO)_3(phen)(py\text{-}3\text{-}NH_2)ClO_4$.

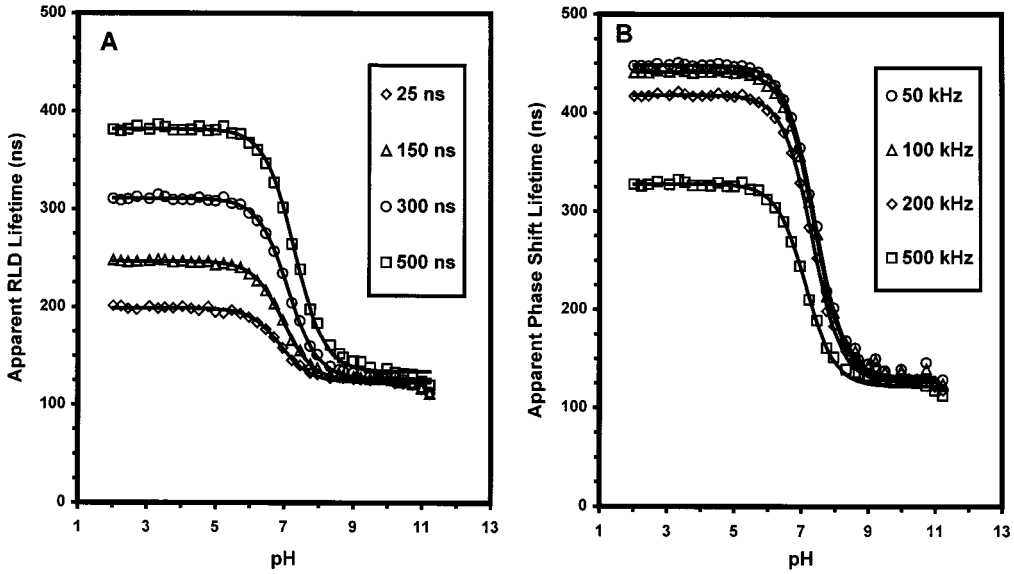

Figure 6. Apparent lifetimes calculated from the measured (α_i, τ_i) parameters shown in Figure 5. (A) RLD lifetimes using a range of gate widths. (B) Phase shift lifetimes using a range of modulation frequencies.

repeated. Two hours was allowed for equilibration between most measurements, and 4 h was allowed between measurements in the pH range from 5 to 9. These long equilibration times were required by the thickness of the films used here, although thinner films can be made that have much faster aqueous diffusion properties. Samples were measured both in the order pH 2 to pH 12 and pH 12 to pH 2. Performing the set of measurements in both directions tends to cancel errors that result from slow diffusion of H^+ and OH^- in the polymer.

RESULTS AND DISCUSSION

Solution-Phase Samples. The emission decay curves obtained from solution phase probe/reference dye mixtures over the pH range 2−11 were fit to a two-component exponential decay equation (eq 5, with $n = 2$), and the data obtained from these fits are shown in Figure 5. The fits for these decay curves returned two lifetimes (τ_P and τ_R) that closely corresponded to the lifetimes of the two complexes measured separately (except at high pH, when the low intensity of the probe made measurements of its lifetime unreliable). The measured preexponential factors for the two components are also plotted as a function of pH. As the figure shows, the two species behave independently with a pH-dependent decrease in α_P (described by eq 12) and a constant value for α_R.

Apparent single-value lifetimes were calculated from the complex decay curves, and the resulting RLD, and phase shift lifetimes are shown in Figure 6. Due to lack of appropriate instrumentation, RLD and phase shift lifetimes were calculated using eqs 6−8 and those in Table 1 and (α_i, τ_i) data obtained from nonlinear least-squares analysis of the decay curves. A range of gate times and modulation frequencies were used to illustrate the effect of these parameters for the determination of apparent lifetimes in multicomponent mixtures. This method gives good approximations to the true RLD lifetimes[16] and should represent good approximations to phase shift lifetimes as well. As the model

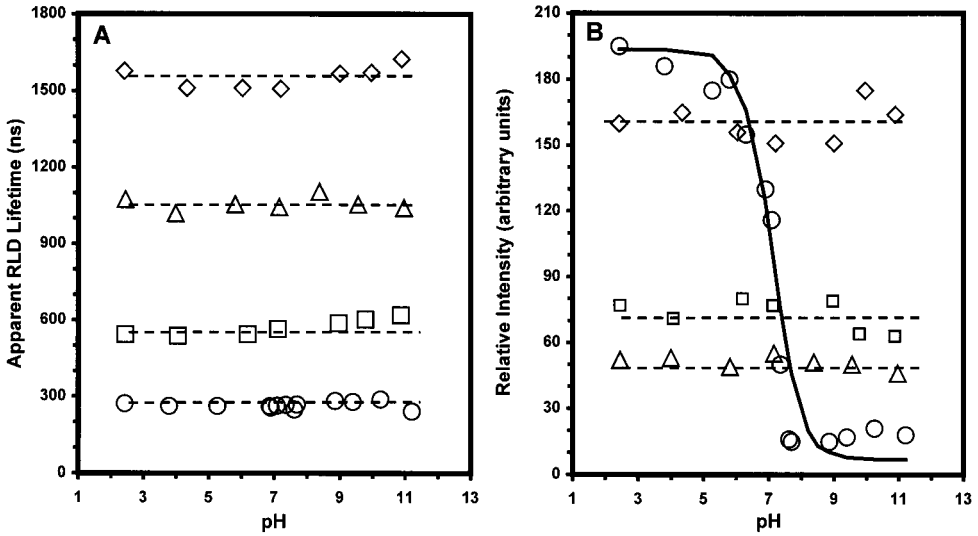

Figure 7. Measured lifetimes (A) and emission intensities (B) of rhenium complexes (○ = $Re(CO)_3(t\text{-but}_2bpy)(py\text{-}3\text{-}OH)ClO_4$, □ = $Re(CO)_3(\phi_2phen)Cl$, △ = $Re(CO)_3(\phi_2phen)(py)ClO_4$, ◇ = $Re(CO)_3(\phi_2phen)(ppp)ClO_4$) in polymer supports. The lifetimes in plot A were calculated from measured (α_i, τ_i) data using a gate time of 500 ns.

Table 4. Photophysical Properties of Rhenium Tricarbonyl Species in Solution and in Polymer Supports

complex	emission max (nm)[a]	solution-phase lifetime (ns)[a]	apparent RLD lifetime in polymer (ns)[b]	pK_a
$Re(CO)_3(t\text{-but}_2bpy)Cl$	590	45	233	na[c]
$Re(CO)_3(\phi_2phen)Cl$	646	270	571	na
$Re(CO)_3(\phi_2phen)(py)ClO_4$	576	4400	958	na
$Re(CO)_3(\phi_2phen)(ppp)ClO_4$	580	3790	1260	na
$Re(CO)_3(t\text{-but}_2bpy)(py\text{-}3\text{-}OH)ClO_4$	568	360	266	6.8[d]
$Re(CO)_3(\phi_2phen)(py\text{-}3\text{-}OH)ClO_4$	578	4040	751	6.6[d]

[a] Measured in nitrogen-purged acetonitrile. [b] Based on data analysis of emission decay curves of doped polymers in aqueous solution and calculated using a gate time of 500 ns. [c] na, not available. [d] Based on intensity measurements of doped polymers in aqueous solution and fit empirically to eq 19.

predicts, the resulting lifetimes are all well-behaved monotonic functions of pH. The apparent pK_a for the two-component mixture was near 7.0 for both lifetime definitions. The results of this solution-phase experiment validate the proposed model for two-dye lifetime-based sensors.

Single-Species Doped Polymer Samples. As expected, all polymer-supported samples, including those with only one luminescent species, exhibited complex emission decays requiring three (α_i, τ_i) pairs for a satisfactory description.[25] RLD lifetimes for these complex decays were calculated for all samples. Although these calculated lifetimes showed a dependence on gate time, the lifetime behavior of all the complexes studied was analogous to that observed in solution in all other respects. The complexes without acidic sites exhibited constant emission intensities and apparent lifetimes over the pH range 2−11, while the hydroxypyridine complexes showed pH-dependent emission intensities. The apparent lifetimes of the hydroxypyridine complexes were constant over the pH range 2−8. Above pH 8, the intensity due to these species is low, and emission decay curves are dominated by noise and impurities, prohibiting reliable lifetime measurements. Representative intensity and lifetime data as a function of pH for rhenium complexes in polymer supports are shown in Figure 7. Measured emission properties for several rhenium complexes in acetonitrile and in polymer supports are summarized in Table 4. The data for polymer-supported samples in this table are based on a typical gate time of 500 ns, although the apparent lifetime of each species does depend on the gate time.

Polymer-Supported Two-Dye Sensors. To evaluate the lifetime response of mixed systems, it is necessary to first comment on the physical validity of the α_i and τ_i parameters that are generated by nonlinear least-squares analysis of complex emission decays. In cases involving a small number (two or perhaps three) of noninteracting luminophores in solution, the (α_i, τ_i) data generated by curve fitting generally correspond to the actual values of the individual components. Such was the case for the solution-phase data presented in Figure 5. For more complex decays, however, such as those observed in polymer-supported systems, there can be no assumption of physical validity for the generated (α_i, τ_i) parameters. A calculated multiexponential decay with three sets of (α_i, τ_i) parameters is usually sufficient to give an accurate description of the measured decay, although the samples may actually contain a very large number of distinct emitting species. In fact, it has been proposed that these systems might be better modeled by a large number of species with a continuous distribution of emission properties.[25] Thus, for polymer samples, the set of (α_i, τ_i) parameters can only be considered as an empirical description of the decay curve. As such, the behavior of the analyte-dependent parameters cannot be subjected to a

(25) Mills, A. *Analyst* **1999**, 1309−1314.

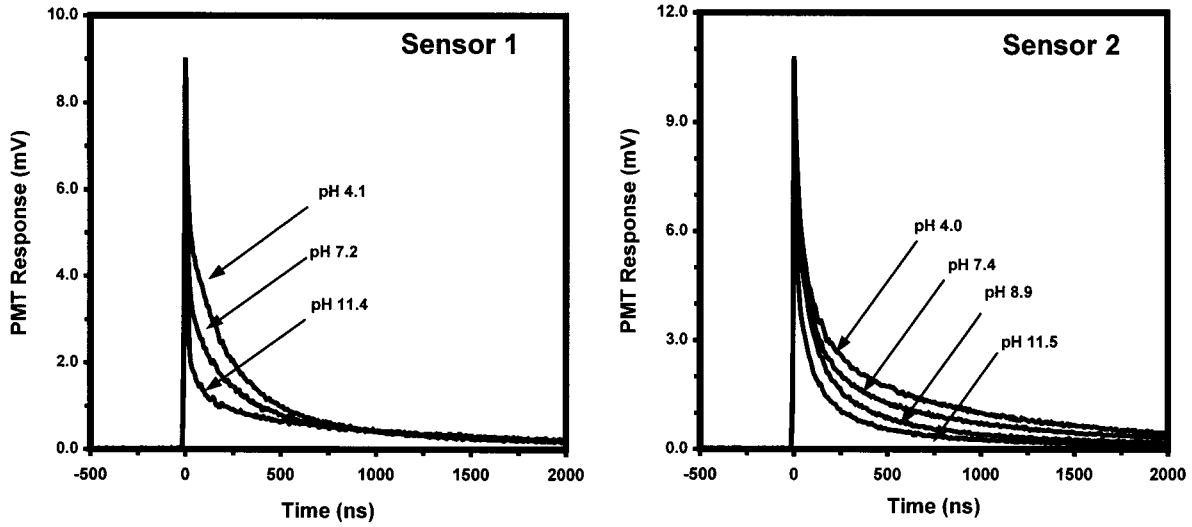

Figure 8. Emission decay profiles of two-component sensors in polymer supports. Sensor 1 employs a short-lived probe, $Re(CO)_3(t\text{-but}_2\text{bpy})(py\text{-}3\text{-}OH)ClO_4$, and a long-lived reference, $Re(CO)_3(\phi_2phen)(ppp)ClO_4$. Sensor 2 uses a long-lived probe, $Re(CO)_3(\phi_2phen)(py\text{-}3\text{-}OH)ClO_4$ and a short-lived reference, $Re(CO)_3(t\text{-but}_2bpy)Cl$. The change in the shape of the decay profiles results from a change in the relative weights of the long- and short-lived components with changes in pH.

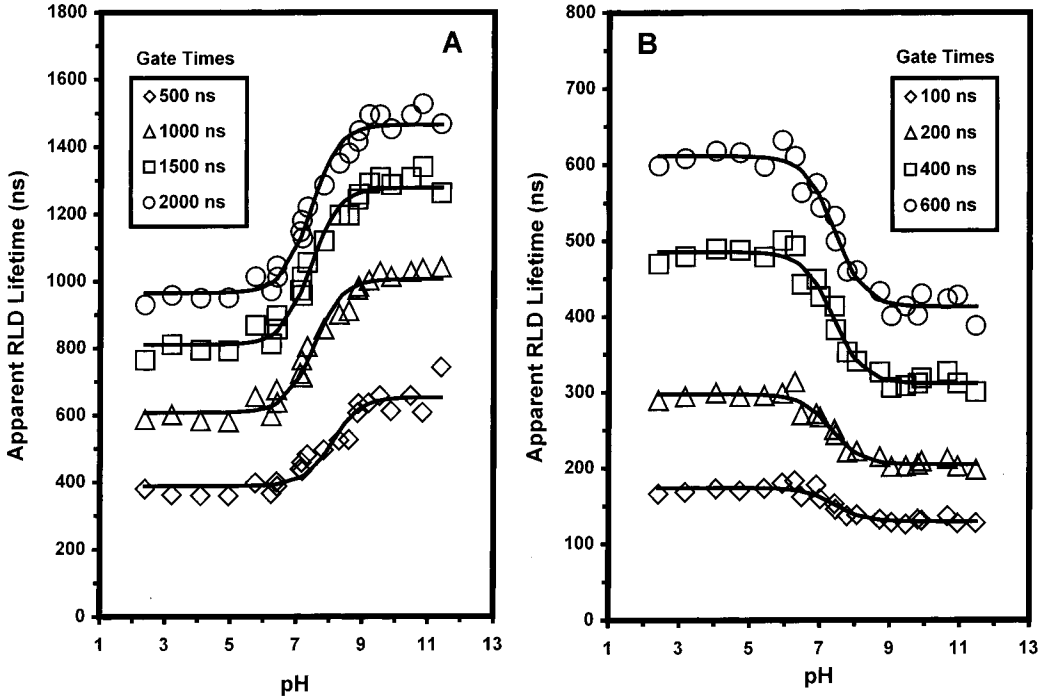

Figure 9. Calculated RLD lifetimes for two-component sensors. The lifetimes were calculated by eqs 6−8, using measured (α_i, τ_i) data.

rigorous mathematical model. One still expects that the emission decay curves for mixed luminophore systems will obey the two-component model qualitatively.

The qualitative behavior of the emission decays of the two-component sensors is shown in Figure 8, which shows measured decay profiles for each sensor in solutions of varying pH. Although both sensors show pH-dependent changes in decay profiles, the nature of the change is different. As the figure shows for sensor 1, which utilizes a short-lived probe and a long-lived reference, increasing pH brings about a dramatic decrease in the earliest portion of the decay curve, while the tail of the decay (beyond ~1000 ns) shows almost no change. This is precisely the behavior that is expected, as the short-lived components contribute less to the overall emission with increasing pH. This is in stark contrast to the behavior of sensor 2, which employs a long-lived probe and a short-lived reference. For this sensor, there is comparatively little change in the early portion of the decay, but a notable decrease in the intensity of the long-lived components. Again, this is the behavior predicted by the two-component model. The emission decay curves of two-component sensors show pH-dependent shape changes brought about by changes in the relative contributions of long- and short-lived components to the overall emission decay.

The most important property to consider for a two-component sensor is the apparent lifetime, which provides a quantitative pH response. Apparent single-value lifetimes as defined by the RLD

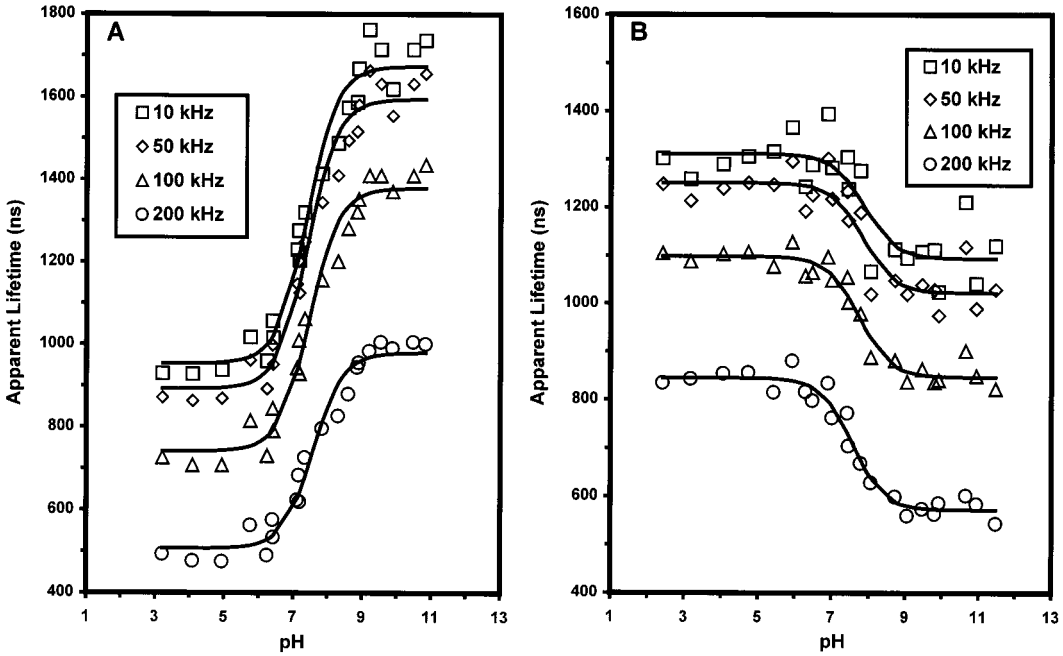

Figure 10. Calculated apparent phase shift lifetimes for two-component sensors. The lifetimes were calculated by the equation in Table 1, using measured (α_i, τ_i) data.

and phase shift methods are shown for both sensors in Figures 9 and 10, calculated using a range of gate times (for RLD) and modulation frequencies (for phase shift). Both sensors exhibited clear changes in apparent lifetimes as a function of pH. The changes were described by smooth monotonic functions. As stated previously, the multiexponential nature of the decays in polymer supports prohibits the application of rigorous mathematical modeling. However, it is found that a well-behaved change in lifetime is obtained and can be fit empirically to a standard two-state titration equation, such as eq 13 in which τ_A and τ_B are the

$$\tau = \tau_A\left(\frac{1}{1+10^{\mathrm{pH}-\mathrm{p}K_a}}\right) + \tau_B\left(1-\frac{1}{1+10^{\mathrm{pH}-\mathrm{p}K_a}}\right) \quad (13)$$

lifetimes in acidic and basic solution, respectively. Effective pK_a values were near 7.0 for all data sets, indicating that these sensors can be used effectively as lifetime-based sensors in the biologically important pH range of 6−8. pH-dependent lifetime behavior is summarized in Table 5. One notes a small but real shift in the apparent pK_a as a function of gate width, which is consistent with the modeled behavior in Figure 4. This shift can be used to tune the effective range of the sensor by varying instrumental parameters.

Table 5. Apparent RLD and Phase Shift Lifetimes for Two-Component Sensors in Polymer Supports

gate time (ns)	τ, acidic (ns)	τ, basic (ns)	$\Delta\tau$ (ns)	effective pK_a
	Apparent RLD Lifetimes: Sensor 1			
500	389	653	264	8.0
1000	608	1006	398	7.5
1500	811	1279	468	7.4
2000	965	1465	500	7.4
	Apparent RLD Lifetimes: Sensor 2			
200	298	205	93	7.3
400	486	312	174	7.4
600	612	413	199	7.4
800	715	518	197	7.5
mod freq (kHz)	τ, acidic (ns)	τ, basic (ns)	$\Delta\tau$ (ns)	effective pK_a
	Apparent Phase Shift Lifetimes: Sensor 1			
10	964	1686	723	7.4
50	892	1594	702	7.4
100	741	1378	638	7.5
200	507	980	472	7.6
	Apparent Phase Shift Lifetimes: Sensor 2			
10	1321	1135	216	7.9
50	1251	1022	229	7.8
100	1098	847	252	7.8
200	845	572	273	7.6

CONCLUSIONS

In this paper, a model is presented for a two-dye lifetime-based sensor. This model represents a new approach to lifetime-based sensing by using a pair of constant-lifetime species, for which one exhibits an analyte-dependent intensity response. The application of this approach allows luminophores that function only as intensity-based sensors to now be used as the active component in lifetime-based sensors as well. This offers several practical advantages including reduced sensitivity to fluctuations in lamp intensity, detector sensitivity, and optical transmission characteristics.

This technique was implemented with mixtures of luminescent rhenium complexes produced as prototypes for two-dye lifetime-based pH sensors. The performance of the sensors was examined both in solution and in polymer supports, both of which showed significant changes in calculated RLD and phase shift lifetimes with pH. These prototype sensors validated the proposed model.

Although the two-dye lifetime-based sensor system described here was used to measure pH in aqueous samples, this technique has wide ranging applicability. Many luminescent species exhibit

analyte-dependent changes in intensity, and any of these can now be used for the fabrication of a lifetime-based sensor.

ACKNOWLEDGMENT

We gratefully acknowledge support by the National Science Foundation (CHE 97-26999 and 00-94777). W.D.B. acknowledges a Dissertation Year Fellowship from the University of Virginia Department of Chemistry.

Received for review October 10, 2001. Accepted February 13, 2002.

AC0110799